Data-Enabled Discovery and Applications (2019) 3: 4
https://doi.org/10.1007/s41688-018-0029-y

ORIGINAL ARTICLE

Wireless High-Resolution Acceleration Measurements for Structural Health Monitoring of Wind Turbine Towers

Bernhard Wondra[1] · Sami Malek[2] · Max Botz[1] · Steven D. Glaser[2] · Christian U. Grosse[1]

Received: 24 October 2018 / Accepted: 21 December 2018 / Published online: 14 January 2019

Abstract

Structural health monitoring (SHM) will be pivotal for safe and economic operation of wind turbines. Timely discovery of changes within the structure and means of prediction of required maintenance will reduce production costs of electricity and catastrophic failures. Long-term structural acceleration recording can support damage detection on turbine towers and document progression of fatigue. Conventional acceleration recordings are based on wired sensor nodes at fixed positions with privileged accessibility and electric power supply. However, such positions might be near vibration nodes and not necessarily experience the maximum vibration amplitude. Shifts in eigenfrequencies can be an indicator of changes in structural stiffness, hence damage, but also be caused by environmental effects, e.g., temperature. Damages generate local effects while the structure's vibration spectrum is a global evaluation. If a sensor is close to the location of damage, the probability of detection is increased. Wireless sensors powered by batteries are advantageous for this task as they are independent of cabling for power supply and data transmission. Such monitoring of turbine tower structures is not common in practice and requires new data-enabled techniques to discover deviations from the optimal way of wind turbine operation. This paper proposes a new approach using wireless high-resolution acceleration measurement sensor nodes, exploiting the vibration response of wind turbine towers. Influences of acceleration resolution and sensor node locations onto the accuracy of eigenfrequency determination are demonstrated. A comparison between acceleration recordings by wireless sensor nodes and their wired counterparts is presented to prove the equivalence of the wireless sensing method. Finally, new data compression techniques used with the sensor nodes are discussed to reduce wireless transmission to a minimum.

Keywords Structural health monitoring · Wireless acceleration measurement · Vibration frequency spectrum · Condition monitoring · Wireless sensor network

✉ Bernhard Wondra
bernhard.wondra@tum.de

Sami Malek
sami.malek@berkeley.edu

Max Botz
max.botz@tum.de

Steven D. Glaser
glaser@berkeley.edu

Christian U. Grosse
grosse@tum.de

[1] Chair of Non-destructive Testing, Technical University of Munich, 81245 Munich, Germany

[2] Department of Civil and Environmental Engineering, University of California, Berkeley, CA 94720-1758, USA

Introduction

In 2017, the wind power capacity installed worldwide exceeded the level of 500 GW [1]. Wind power is becoming the dominant renewable source of energy in the European Union and generated more than 10% of its electricity [2]. Due to the large number of installed wind turbines and the standard design lifetime of 20 years, a large percentage encounters its end of service life within the next few years. However, not every wind turbine experienced the load conditions assumed at its design, but preserved significant remaining useful lifetime (RUL). Research projects such as the MISTRALWIND project aim at the extension of the RUL [3]. To warrant a safe long-term operation of wind turbines and to predict the RUL from the evolvement of fatigue, changes in the structural integrity need to be detected, analyzed, and

recorded continuously. Such permanent SHM provides several advantages. It enables complete insight into the load history and its subsequent influence on the building's behavior. Maintenance periods can be extended, depending on the real condition of individual components, and replacements can be synchronized with planned plant's downtime at predicted low wind periods. In case a significant RUL is found at the end of initially warranted service life, an extension of operation permit can be applied for, supported by recorded SHM data. In addition, a SHM sensor network can also contribute to the optimization of the wind turbine's operation as well as to a more efficient and cost-optimized maintenance. Sophisticated sensor networks are capable of warning the turbine's control system of excessive loads during periods of high wind speeds and can recommend a change of operation strategy. Maintenance teams could evaluate the recorded data prior to planned inspection and determine potential hotspots of expected fatigue.

Two of the most common sensor types utilized for wind turbine tower monitoring are strain gauges and acceleration measurement sensors. Conventional strain gauges were used for long-term monitoring and damage detection, thus aiming at the extension of service life [4, 5]. Noppe et al. showed that a short-term recording by use of strain gauges and a subsequent training of neural network plus exploitation of Supervisory Control and Data Acquisition (SCADA) data can also contribute to fatigue assessment [6]. Wire-based acceleration measurement sensors were used by Smarsly et al. for onshore turbine structure monitoring [7]. Weijtjens et al. used accelerometers for monitoring of offshore wind turbines with special attention to the foundation [8]. Wire-based sensors are typically installed at distinct locations on the tower wall with easy access to installed electricity supply, usually the platforms or the nacelle. Another limitation is the need for connection of sensors to a data acquisition unit by cables. Such locations experience a dynamic response to the wind forces, but alternative positions can receive larger vibration amplitudes and thus be more suited to achieve a higher signal-to-noise ratio. Ideally, a sensor network would feature one sensor at every antinode of each vibration mode.

Wireless acceleration measurement sensors are independent of electric respectively data transmission cables. Swartz et al. used wireless accelerometers already in 2008 for wind turbine monitoring [9]. Recent high-resolution wireless acceleration sensors have proven to detect even tiny vibrations of bridges [10]. Most acceleration recordings strive at an evaluation of a vibration spectrum and a shift of eigenfrequencies, indicating a change of structural stiffness, i.e., potential damage. However, the vibration spectrum contains a global representation of a structure, while damages achieve local effects [11]. The closer a sensor to a damage location, the higher the probability to detect the local effect. Pandey et al. proved that a change of flexural mode can indicate a damage [12]. The curvature/strain modes method takes advantage of this approach. The flexibility of wireless sensors with respect to mounting positions on the tower structure supports this strategy. Still the wireless sensors need to feature a high resolution to detect the low accelerations at low wind speed, even at low frequencies. For instance, first bending modes at offshore wind turbines can be significantly lower than 0.2 Hz [13].

This paper presents the concept of wireless high-resolution acceleration sensors for exploitation of a wind turbine tower's vibration response. Two types of wireless acceleration sensors are utilized with different measurement resolution, thus the impact of measurement resolution on the eigenfrequency determination can be demonstrated. The tested wind turbine was also instrumented with wire-based acceleration sensors which enables a comparison of wireless sensor data to recordings received from wire-based counterparts.

Wireless sensors require an autonomous power supply, for instance a battery. Due to the limited energy storage, transmission of data via antenna needs to be reduced to achieve long-term uninterrupted operation. Recorded raw acceleration data can be compressed on the sensor chip and then transferred to a gateway. One way of data compression is a fast Fourier transform (FFT) of the raw data on the sensor chip to generate a frequency spectrum, followed by a peak-picking procedure of the eigenfrequencies with highest amplitudes and finally transmission of these frequencies plus their related amplitudes only. In this work, raw acceleration data is first recorded, transmitted, and then converted externally to find the most suitable process of data compression. This data compression method will be embedded in a subsequent study on the sensor firmware to compress the raw data and to transmit only the key information.

This paper describes the studied wind turbine and the wireless acceleration measurement sensor nodes plus the data compression techniques in the "Materials and Methods" section. Wireless acceleration measurement campaigns and the comparison to signals recorded by wire-based measurement instruments are outlined in the "Wireless Acceleration Measurements" section. Results are discussed in "Results and Discussion" section, while the "Conclusions" section refers to the conclusions.

Materials and Methods

Description of Studied Wind Turbine and Response of Tower Structure to Forces

The studied wind turbine is a 3-MW 3-bladed horizontal axis wind turbine (HAWT), located in Bavaria, Germany

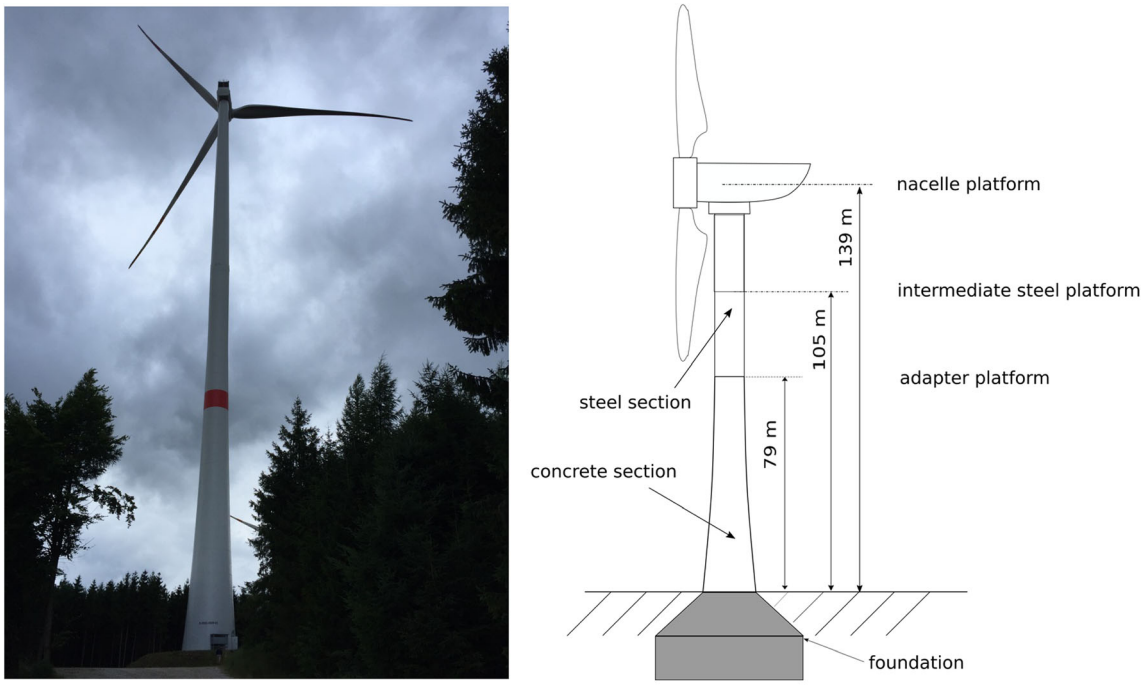

Fig. 1 Studied wind turbine: **a** photo of wind turbine under operation and **b** sketch of wind turbine and platforms heights

(Fig. 1). Its support structure is a hybrid concrete-steel tower with a hub height of 140 m, carrying a rotor of 113-m diameter. Both rotor mass and nacelle-generator mass are 70 tons each, resulting in a total weight of 140 tons on top of the tower structure. The lower concrete section and the upper steel section are interconnected 79 m above ground. At this height, there is an adapter platform for easy inspection and maintenance access to the prestressed tendons. Two further platforms are part of the tower structure: the intermediate steel platform 105 m above ground and the nacelle platform 139 m above ground. All these platforms provide easy access for implementation of acceleration sensors and suitable electric supply for instrumentation. Via the integrated lift, even mounting positions on the inner tower wall between the platforms can be reached. Wire-based acceleration sensors are installed at the adapter platform, the nacelle platform and at the inner tower wall at heights of 45 m (concrete section) and 112 m (steel section). All wire-based acceleration sensors feature a three-dimensional recording with a typical broadband resolution of 0.25 mg rms. Data transfer from the wire-based sensors to the PC at the ground is performed via optical cables. To account for the influence of thermal changes, temperature sensors were installed both at the adapter platform and the nacelle platform.

Wireless sensors benefit from a free line-of-sight to the receiver of the gateway. Both the adapter platform and the intermediate steel platform include a center opening for the lift. At the center of the nacelle platform, there is an opening for the power cables which conduct the electricity from the generator to the grid connection at the ground. Thus, wireless transmission with a free line-of-sight is possible in case the antennas of the wireless sensors are installed close to these openings.

The vibrational response of the tower is similar to the one of a cantilever beam. Bending in fore-aft direction mainly results from the wind thrust parallel to the rotor axis, bending in side-side direction results from eccentric rotating masses, e.g., ice on the rotor blades, or turbulent wind excitation, and torsion around the vertical tower axis is caused by yaw maneuvers or non-symmetric horizontal distribution of wind onto the rotor [14]. During turbine operation at its nominal rotation speed of 14 rpm, the rotational frequency (1 per revolution, 1p) of 0.23 Hz and the blade passing frequency (3p) of 0.7 Hz as well as higher harmonic oscillations can appear in the frequency spectra derived from the measurement data.

Wireless Sensor Nodes and Data Compression Technique

Description of Wireless Acceleration Measurement Sensor Nodes

For this study, wireless sensor nodes “Neomote” and the referring gateway “Network Manager” from Metronome Systems LLC were utilized. These instruments and the data acquisition software have been developed and enhanced by

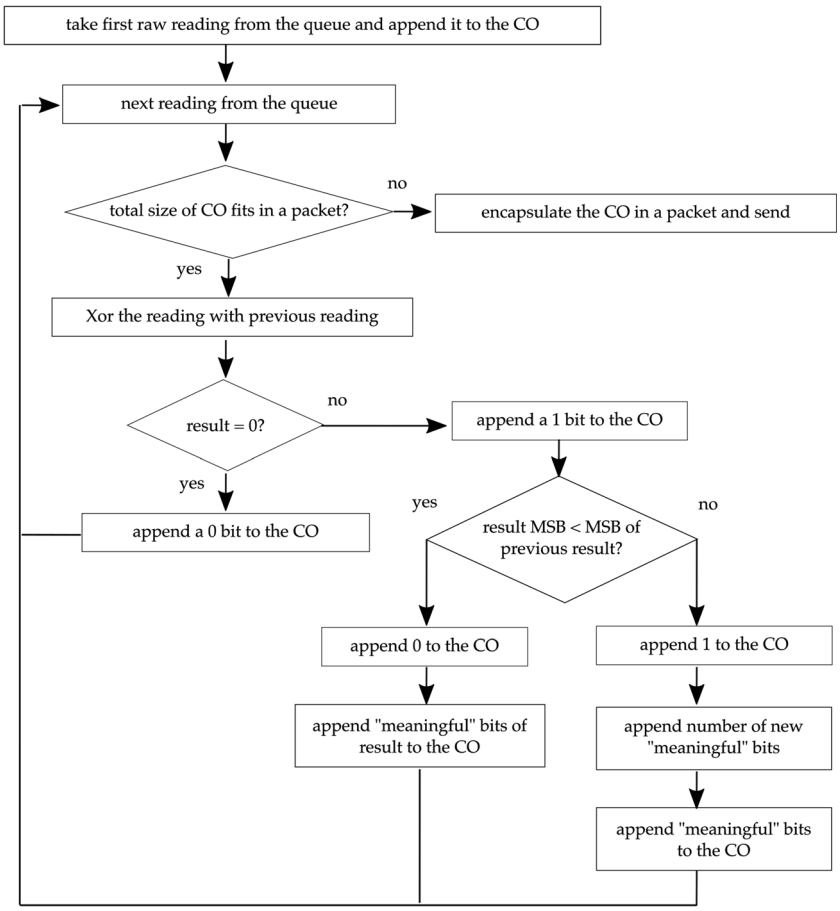

Fig. 2 Algorithm of data compression technique. CO denotes compressed output and MSB denotes most significant bit

Prof. Steven Glaser, University of California, Berkeley [15]. The hardware generation dated 2016 utilized the MEMS based acceleration sensor chip ADXL 362 from Analog Devices [16]. It features a settable measurement range of ± 2, 4, or 8 g and a 12-bit resolution of the recorded value, which results in an acceleration resolution of ± 1 mg at the lowest settable acceleration range of ± 2 g. Accelerations beyond 2 g at a wind turbine tower are very unlikely, so the acceleration range was adjusted to ± 2 g. The sampling frequency can be adjusted from 12.5 to 400 Hz in steps (i.e., 12.5, 25, 50, …). The software of the first sensor node generation provided the choice to transmit either raw acceleration data or FFT converted signal or both, the option to record acceleration values either in one or three dimensions. To comprehensively understand the typical loads applied by the varying wind forces over time, the sensor nodes were set for transmission of complete raw acceleration data. Such data was exploited and analyzed first before an ideal conversion on the sensor chip could be selected.

The second hardware generation dated fall 2017 is based on the ADXL355 sensor chip from Analog Devices [17], a three-axis MEMS accelerometer with settable ranges of ± 2, 4, or 8 g. At the ± 2 g range, the sensitivity is 256,000 LSB/g, which results in a scale factor of 3.9 μg/LSB. Sampling rates of the sensor node can be set wirelessly to 3.9 Hz, 7.8 Hz, 15.6 Hz, or 31.25 Hz. Higher sampling rates can be set, but

Table 1 Example of "constant readings" case

Acceleration reading sample	Binary representation	Xor result	Case	numBits CO	MSB location	Bits saved
5	"00000101"	N/A	N/A	8	− 1	0
5	"00000101"	"00000000"	0	1	− 1	7
5	"00000101"	"00000000"	0	1	− 1	7
5	"00000101"	"00000000"	0	1	− 1	7
5	"00000101"	"00000000"	0	1	− 1	7
						28

Table 2 Example of "typical readings" case

Acceleration reading sample	Binary representation	Xor result	Case	numBits CO	MSB location	Bits saved
2	"00000010"	N/A	N/A	8	−1	0
6	"00000110"	"00000100"	11	2 + S + 3	2	0
4	"00000100"	"00000010"	10	2 + 3	2	3
8	"00001000"	"00001100"	11	2 + S + 4	3	−1
1	"00000001"	"00001001"	10	2 + 4	3	2
						4

exceed the wireless receiving rate at the gateway, i.e., in case 3 sensor nodes with simultaneous recordings of 3 axes each at frequency of 31.25 Hz are performed.

Data Compression Technique

The manager that collects data from the accelerometers has a maximum reception threshold of 32 packets per second assuming perfect connection quality. When the wireless network surpasses this rate, packets will be lost. With maximum effective packet size of 90 bytes, sample size of 3 bytes and 3 axes sampling mode, this translates into a maximum reception rate of 320 samples per second assuming no protocol packet overhead. If a faster rate is needed for multiple sensors, each sensor can record for the needed time, sequentially. Since the system is stationary this is not a problem. If one wishes to use 5 motes for instance, the theoretical maximum sampling frequency they can use is 64 Hz. To increase the system's capability, we implemented a data compression algorithm based on the time series database compression scheme of Gorilla [18] for the wireless sensors of second hardware generation. Raw accelerometer readings are first stored in a queue at the mote side and once a certain queue size threshold is reached, the encapsulation into packets begins. The compression algorithm for every packet to be created is as shown in Fig. 2:

At the beginning, the first raw reading is taken from the queue and appended to the compressed output (CO). For each subsequent reading, while the total size of the CO fits in a packet, an exclusive-or (Xor) comparison of the reading with the previous reading is performed. If the result equals 0, a 0 bit is appended to the CO. Otherwise, a 1 bit is appended to the CO, followed by case discrimination with respect to the most significant bit (MSB): If the result's MSB is less than that of the previous result, a 0 bit is appended to the CO and the "meaningful" bits of the result are appended to the CO. Otherwise (i.e., if the result's MSB is greater than that of the previous result), a 1 bit is appended to the CO, the number of the new "meaningful" bits is appended and then the "meaningful" bits are appended to the CO. When the maximum size of the CO is reached, the CO is encapsulated in a packet and sent.

The best-case scenario for such algorithm is when all samples have the same value. This translates into a total of 697 samples in 1 packet versus the non-compressed case with 30 samples per packet. In worst case scenarios, however, the compressed output could yield a lower number of samples compared to the non-compressed one. To help avoid such cases, we need to avoid sudden differences in significant bits. We apply an offset to the accelerometer readings to make sure all samples to be compressed are positive, thus avoiding the 2's complement representation. Worst cases should now occur when either there is a maximum sensor magnitude change (~ 27 samples per packet), or when the magnitude keeps increasing at a power of 2 rate per sample (~ 20 samples per packet). The compression process is restarted for every packet, which mitigates the negative effects of such cases. Tables 1, 2, 3, 4, and 5 illustrate the effect of different example scenarios on the number of bits saved compared to the reference scheme of no compression for an 8 bit sample size. S is the number of bits needed to store the length value of meaningful bits and is equal to log2(8) = 3 for samples of size 8 bits. The "case" column indicates the prefix bits added to the CO as explained

Table 3 Example of "power of 2 increase readings" case

Acceleration reading sample	Binary representation	Xor result	Case	numBits CO	MSB location	Bits saved
4	"00000100"	N/A	N/A	8	−1	0
8	"00001000"	"00001100"	11	2 + S + 4	3	−1
16	"00010000"	"00011000"	11	2 + S + 5	4	−2
32	"00100000"	"00110000"	11	2 + S + 6	5	−3
64	"01000000"	"01100000"	11	2 + S + 7	6	−4
						−10

Table 4 Example of "shock readings" case

Acceleration reading sample	Binary representation	Xor result	Case	numBits CO	MSB location	Bits saved
0	"00000000"	N/A	N/A	8	−1	0
1	"00000001"	"00000001"	11	2 + S + 1	0	2
64	"01000000"	"01000001"	11	2 + S + 7	7	−4
0	"00000000"	"01000000"	10	2 + 7	7	−1
2	"00000010"	"00000010"	10	2 + 7	7	−1
						−4

in Fig. 2. "numBits CO" column shows the number of bits added to the CO for each sample. MSB column indicates the location of the most significant bit. Note that MSB only changes when new MSB of Xor is bigger than the previous MSB of Xor. Note that for the Negative value, Shock, and the Power of 2 increase cases, the total negative bits saved values indicate that it is more beneficial not to compress.

Wireless Acceleration Measurements

Measurement Campaign of Wireless Sensor Nodes First Hardware Generation at Studied Wind Turbine

On July 12, 2017, tests of the wireless sensor nodes of first generation were performed on the studied wind turbine. This measurement campaign took advantage of an easy installation at the adapter platform and the nacelle platform. One wireless sensor node and the receiving gateway were installed on the adapter platform. Two sensor nodes were mounted on the nacelle platform close to the platform opening for the generator's power cables, the sensor nodes' antennas directed towards the lower platforms to achieve a free line-of-sight for radio transmission to the receiving gateway on the adapter platform. Signals from all sensor nodes were received and stored at the receiving gateway. The acceleration range was set to ± 2 g, three-dimensional acceleration measurement was used and raw data transmission mode was chosen. During this campaign, the sampling frequency per axis of the sensor nodes was set to 12.5 Hz due to several reasons: Most eigenfrequencies of the studied tower structure are expected to be below 6.2 Hz and the design frequency of the first bending mode is less than 0.3 Hz. The simultaneous usage of three sensor nodes with acceleration recordings in three dimensions each resulted in a total data transmission of 112 Hz. Sampling frequencies of 50 Hz per axis or higher would have exceeded the maximum receiver frequency and resulted in loss of data.

During a first measurement period of 20 min, the wind speed was moderate (max. 15 m/s at 140 m altitude). At the adapter platform, the maximum acceleration in horizontal directions and vertical direction did not exceed 7 mg. At the nacelle platform, the acceleration in vertical direction was limited to 5 mg and the accelerations in horizontal directions to 10 mg (Fig. 3). The acceleration signals were recorded and the corresponding frequency spectrum was determined during postprocessing using fast Fourier transform (FFT).

After a short break, a second measurement period for 2 h started. During this period, the wind speed increased up to 24 m/s at 140 m altitude. Acceleration values in vertical direction were still limited to 7 mg at both platforms. Horizontal accelerations (fore-aft and side-side) reached 20 mg at the adapter platform and 30 mg at the nacelle platform (Fig. 4), except for a short period with 50 mg in horizontal direction at the adapter platform.

These measurements demonstrate that even high wind speeds result in acceleration values only one order of magnitude above the sensor's resolution limit. Discretization steps can be seen when the acceleration was only a few mg. Because of this, a higher sensor resolution is advantageous.

Table 5 Example of "negative value" case

Acceleration reading sample	Binary representation	Xor result	Case	numBits CO	MSB location	Bits saved
5	"00000101"	N/A	N/A	8	−1	0
6	"00000110"	"00000011"	11	2 + S + 2	1	1
−1	"11111111"	"11111001"	11	2 + S + 8	7	−5
2	"00000010"	"11111101"	10	2 + 8	7	−2
0	"00000000"	"00000010"	10	2 + 8	7	−2
						−8

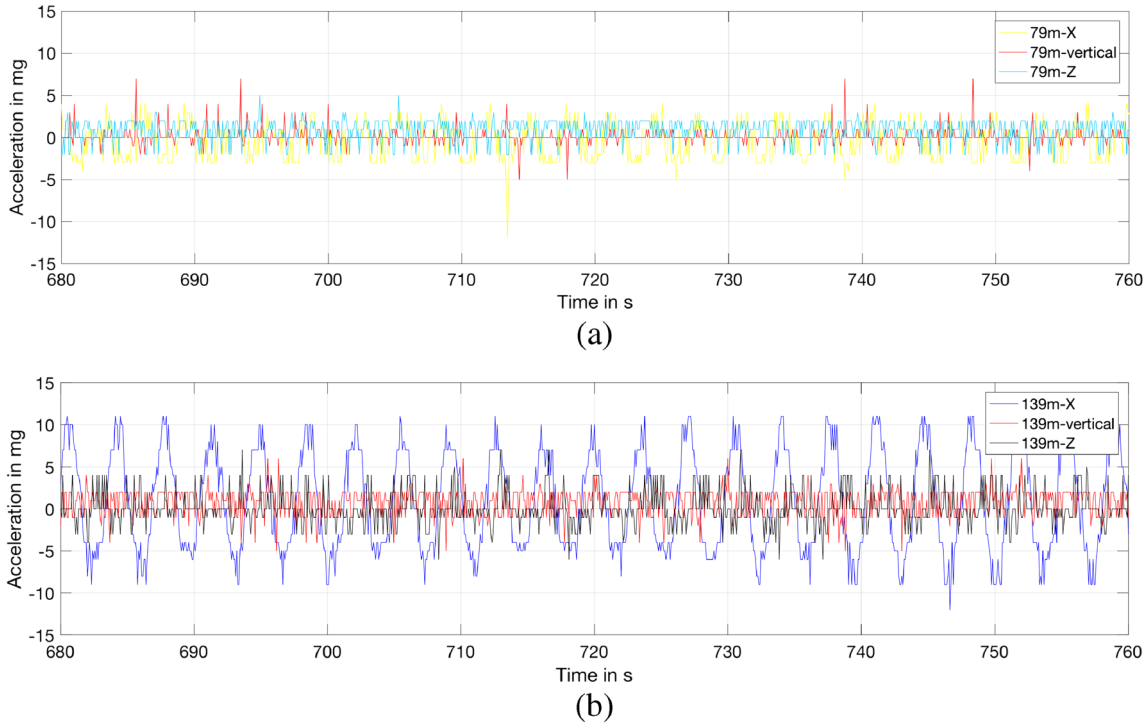

Fig. 3 Accelerations measured during first period (20 min): **a** on adapter platform and **b** on nacelle platform

Noise measurement of Wireless Sensor Nodes Second Hardware Generation

According to the data sheet for the ADXL 355 sensor, the sensitivity is specified to 3.9 µg/LSB at the lowest settable acceleration range of ± 2 g. The measurement noise on system level can be higher and needs to be tested to confirm a sufficiently high resolution for the wind turbine tower monitoring. Three wireless sensor nodes of second hardware generation were put on the ground of a building in absence of any vibrating devices. The sampling frequency was set to 31.25 Hz, three-dimensional recording was activated and the acceleration range of ± 2 g was chosen. The sampled acceleration values were recorded for a period of 550 s. As shown in Fig. 5, the recorded values did not exceed 200 µg. The calculated standard deviation for all three sensors was 42–43 µg for the *X*- respectively *Y*-direction and 59–63 µg for the *Z*-direction.

Measurement Campaign of Wireless Sensor Nodes Second Generation at Vibration Test Station

To examine the performance of the new hardware generation, these sensor nodes were tested on a vibration test station at the facilities of IABG mbH, Ottobrunn, Germany. The vibration test station consists of a 5-m vertical steel tube, equipped with several wire-based acceleration sensors of high resolution (0.1 mg) and high sampling rate (1 kHz), an eccentric motor and a sine wave generator. More than ten wired sensors for acceleration recording in *X*-direction and the same number of wired sensors for *Y*-direction are distributed along the tube height. The eccentric motor uses a load of 1.4 kg on a lever and is mounted on a plate on top of the steel tube. At the side of the steel tube, a metal frame carries a sine wave generator 1.7 m above ground. The sine wave generator is linked to the steel tube by a steel rod (Fig. 6b).

Three wireless sensor nodes of the second generation were mounted on the vibration test station: one was mounted on the plate on top of the steel tube, one at the steel tube approx. 3.5 m above ground (Fig. 6a) and one sensor node on the steel tube itself approximately 1.8 m above ground. Different frequencies of the eccentric motor (1 Hz, 2.5 Hz, 4 Hz) and of the sine wave generator (3 Hz, 7.5 Hz, 12 Hz, forces from 290 to 570 N peak-to-peak) were applied to the steel tube, whilst both the wireless sensor nodes and the wire-based counterparts recorded the accelerations. The load conditions lasted between 30 and 120 s. Some tests included a stop of eccentric motor, simulating an emergency stop, plus a stop of the sine wave generator to achieve a free oscillation of the steel tube with decaying amplitude.

Measurement Campaign of Wireless Sensor Nodes Second Hardware Generation at Studied Wind Turbine

On March 28, 2018, the wireless sensor nodes of the second generation were installed at the wind turbine. One sensor node

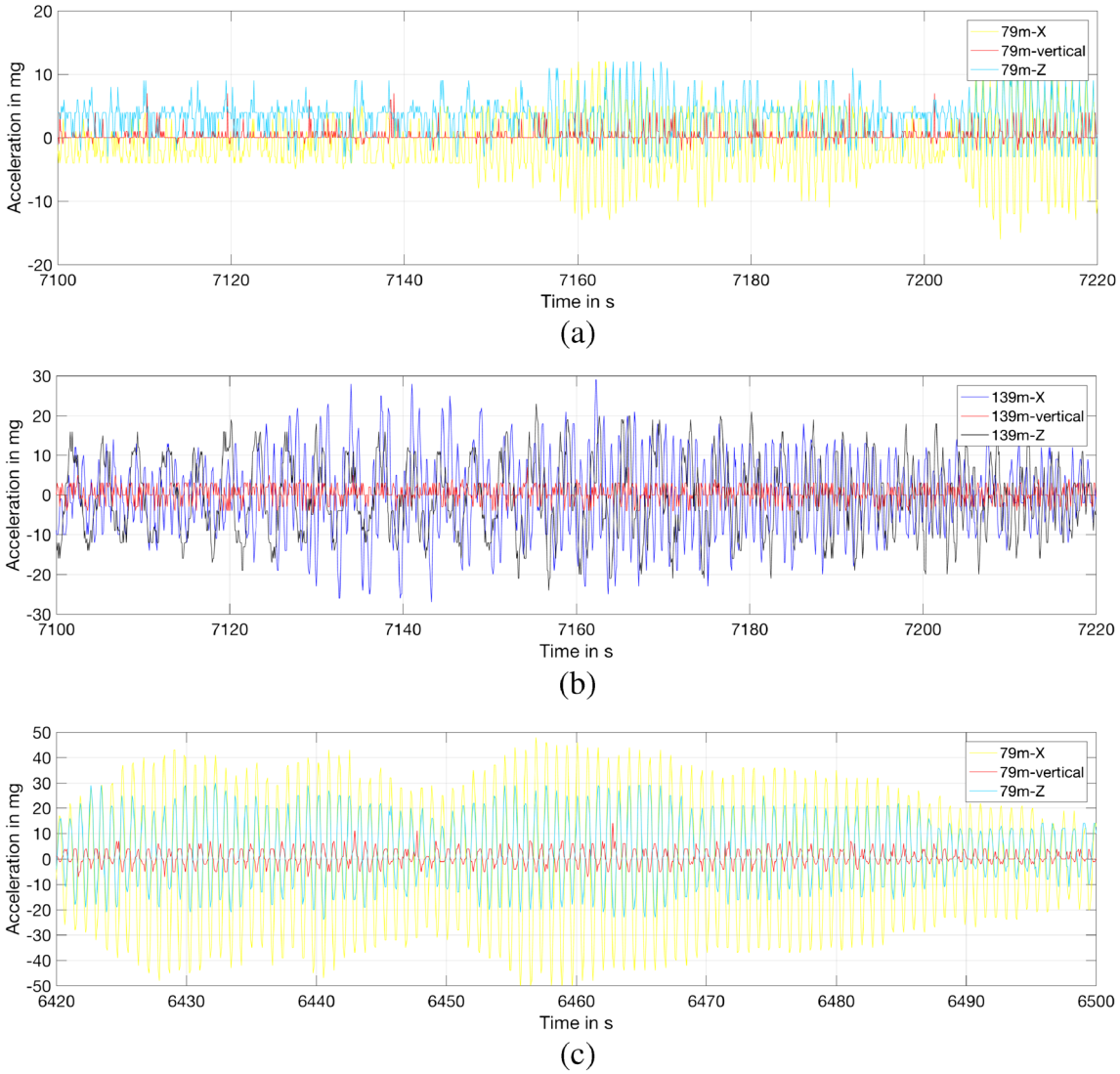

Fig. 4 Accelerations measured during second period (2 h): **a** on adapter platform, **b** on nacelle platform, and **c** on adapter platform with maximum acceleration for very short period

was installed at the nacelle platform, one at the intermediate steel platform and one on the adapter platform. The receiving gateway was installed at the adapter platform to reduce the transmission distance. Two measurement periods took place, the first one lasting 1 h 25 min and the second one lasting 1 h. Wind speed during these periods varied between 5.1 and 11.5 m/s. During the first period, acceleration values up to 50 mg were measured, as shown in Fig. 7.

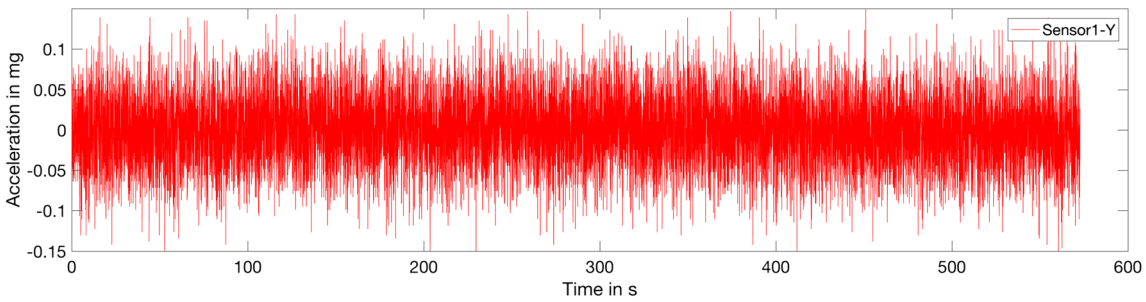

Fig. 5 Acceleration measurement of wireless sensor node second hardware generation in Y-direction during absence of movement

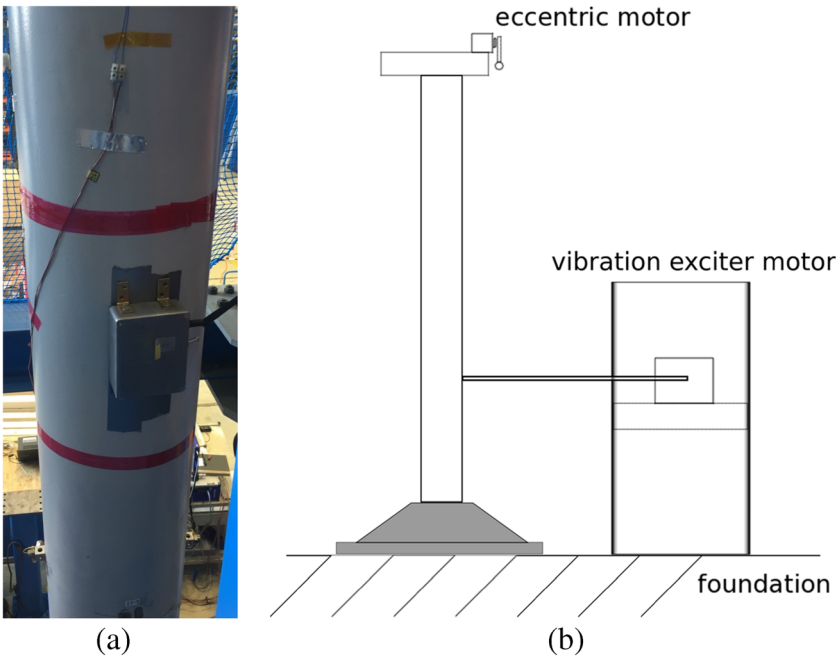

Fig. 6 Vibration test station: **a** sensor node of second hardware generation mounted on steel tube at 3.5 m above foundation and **b** sketch of vibration test station

Comparison to Installed Wire-Based Accelerometers

A stationary monitoring system was installed in the tower of the studied wind turbine in January 2016. Nearly uninterrupted measurement data with a sampling frequency of $f_s = 625\ Hz$ is available since then. The monitoring system consists of several wire-based accelerometers (PCB 3713B112G from PCB Piezotronics), a seismometer, strain gauges and thermocouples. More details on the monitoring system can be found in [19–21]. The accelerometers are installed at the adapter platform and the nacelle platform, as well as at the inner tower wall at heights of 45 m and 112 m. The acceleration range of this wire-based sensor type is ± 2 g. As the measurement is running continuously, simultaneous data is available that can be compared to the wireless acceleration measurements.

For that purpose, signals from sensors at the same position with the same orientation are needed. The stationary sensors on different levels are not oriented equally due to varying boundary conditions. In a first preprocessing step, the measurement data is transformed to a common, tower-fixed coordinate system. During the measurement campaign using wireless sensor nodes of second hardware generation at the wind turbine, the sensor nodes were oriented nearly equally with the x-axis pointing towards the tower entrance door. The coordinate system of the stationary sensors was consequently transformed to match this orientation. Figure 8 shows the horizontal acceleration signals at 79 m tower height obtained by wired and wireless accelerometers.

The acceleration signals from these two independent measurement systems were found to be consistent for both measurement periods on March 28, 2018, for all three positions. However, the data obtained by the wireless sensor nodes showed a time/sampling frequency shift over the measurement period. The signals were synchronized so that the first peak occurs at the same time. At the end of the measurement period, there is a time lag of several seconds. This time lag varies for each sensor. A comparison of the internal counter of each wireless sensor in each direction and the related number of transmitted data sets received by the gateway indicated a loss of data depending on the measurement period, the sensor and the axis direction. For the first period, the loss of transmitted data varied from 2.3 to 6.3%. During the second period, the loss of recorded data was max. 0.3%. As such loss of data does not have to be distributed equally over time, the set sampling rate of 31.25 Hz was used for the comparison of wirelessly recorded data to the wire-based counterparts. When converting the time series of acceleration values from the second period by FFT, the small loss of recorded data (max. 0.3%) will result in a very small deviation of eigenfrequencies from the ones derived from a time series without loss of recorded data. The loss of data from the first period can have a bigger impact, depending on how this loss is distributed.

Results and Discussion

Results from Measurement Campaign of Wireless Sensor Nodes First Generation at Wind Turbine

During the first test period on July 12, 2017, the wind speed was moderate, thus the accelerations were limited to a few mg. The frequency spectra in horizontal directions showed the

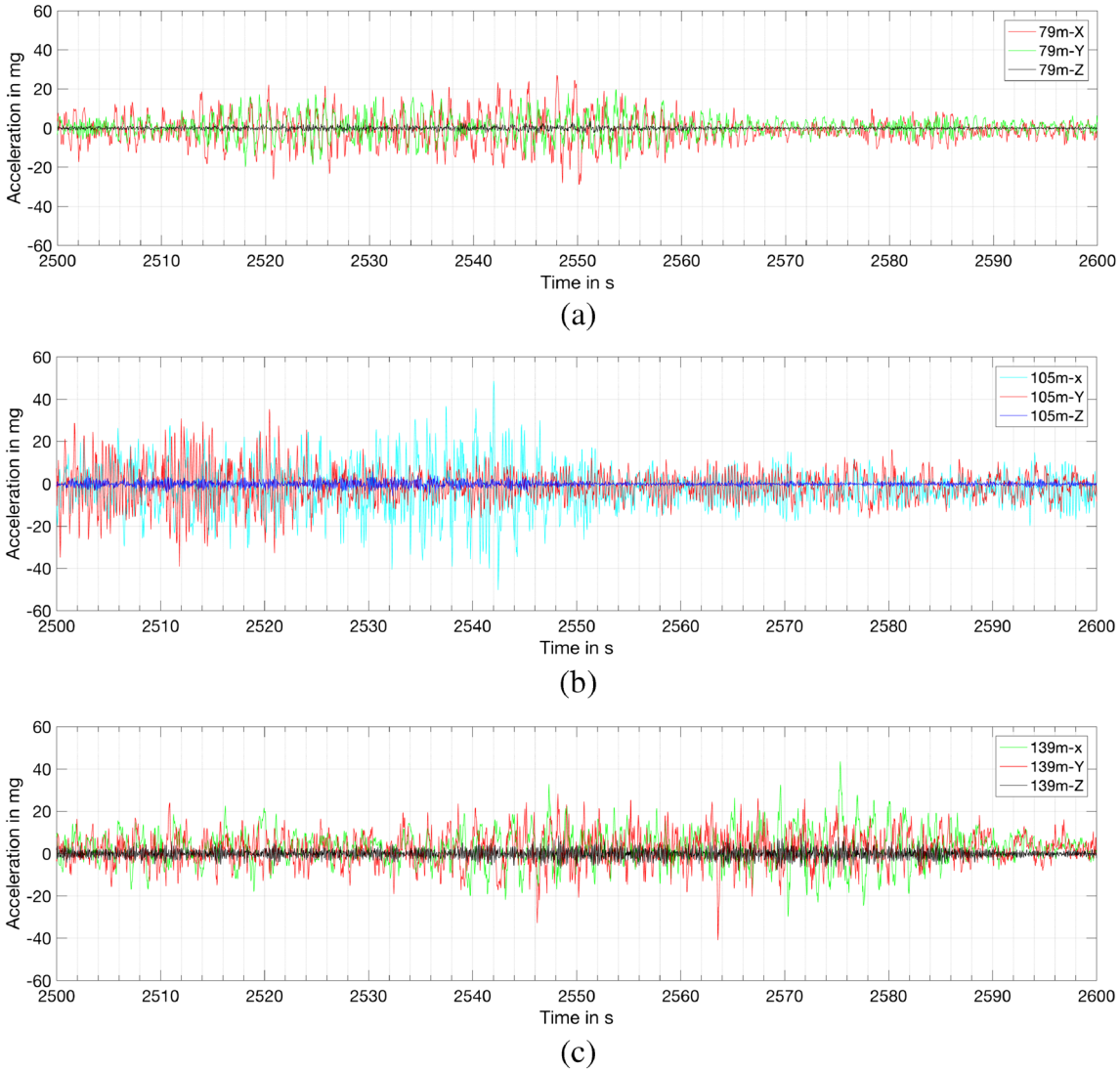

Fig. 7 Measured accelerations during first period at three platforms in *X*-, *Y*-, and *Z*-direction: **a** on adapter platform, **b** on intermediate steel platform, and **c** on nacelle platform

expected first bending eigenfrequency at 0.27 Hz, but no further significant eigenfrequency (Fig. 9a).

During the second test period on the same day, the wind speed increased up to 24 m/s at the nacelle height and the

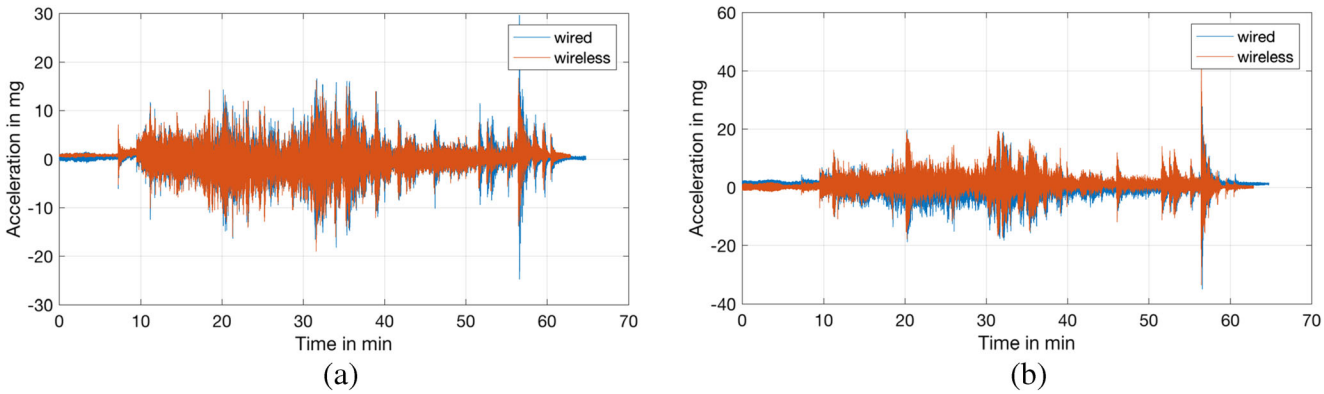

Fig. 8 Acceleration signals obtained by wired and wireless measurements on 28 March 2018 at wind turbine, 79 m height: **a** *X*-direction and **b** *Y*-direction

recorded accelerations were significantly higher. The subsequent exploitation of the recorded acceleration values in horizontal directions showed again the first bending frequency at 0.27 Hz, but additionally three further frequencies (Fig. 9b): One at 0.85 Hz with an amplitude ten times smaller than the first bending frequency, one at 1.09 Hz with an amplitude of two thirds of the first bending frequency, and one at 1.17 Hz with a comparable amplitude to the one at 0.85 Hz. The transform of signal in vertical tower axis from time domain to frequency domain from the first period did not show significant eigenfrequencies. Even the first bending frequency was nearly hidden by the noise floor. The FFT of acceleration signals in vertical direction from the second period (Fig. 9c) showed two significant frequencies at 0.27 Hz and 1.09 Hz. No further eigenfrequencies were observed in the spectrum derived from the vertical accelerations. However, there are tolerances of alignment for the wireless sensor nodes. There can be some small proportion of horizontal acceleration signals into the vertical recording. The movement in vertical direction is small compared to the horizontal displacements, thus influence of an axis misalignment cannot be excluded.

Results from Measurement Campaign of Wireless Sensor Nodes Second Generation at Vibration Test Station

The accelerations up to 1.5 g and the eigenfrequencies measured at the vibration test station were remarkably higher than the ones measured at common wind turbines. This test was intended to compare the performance of the second generation

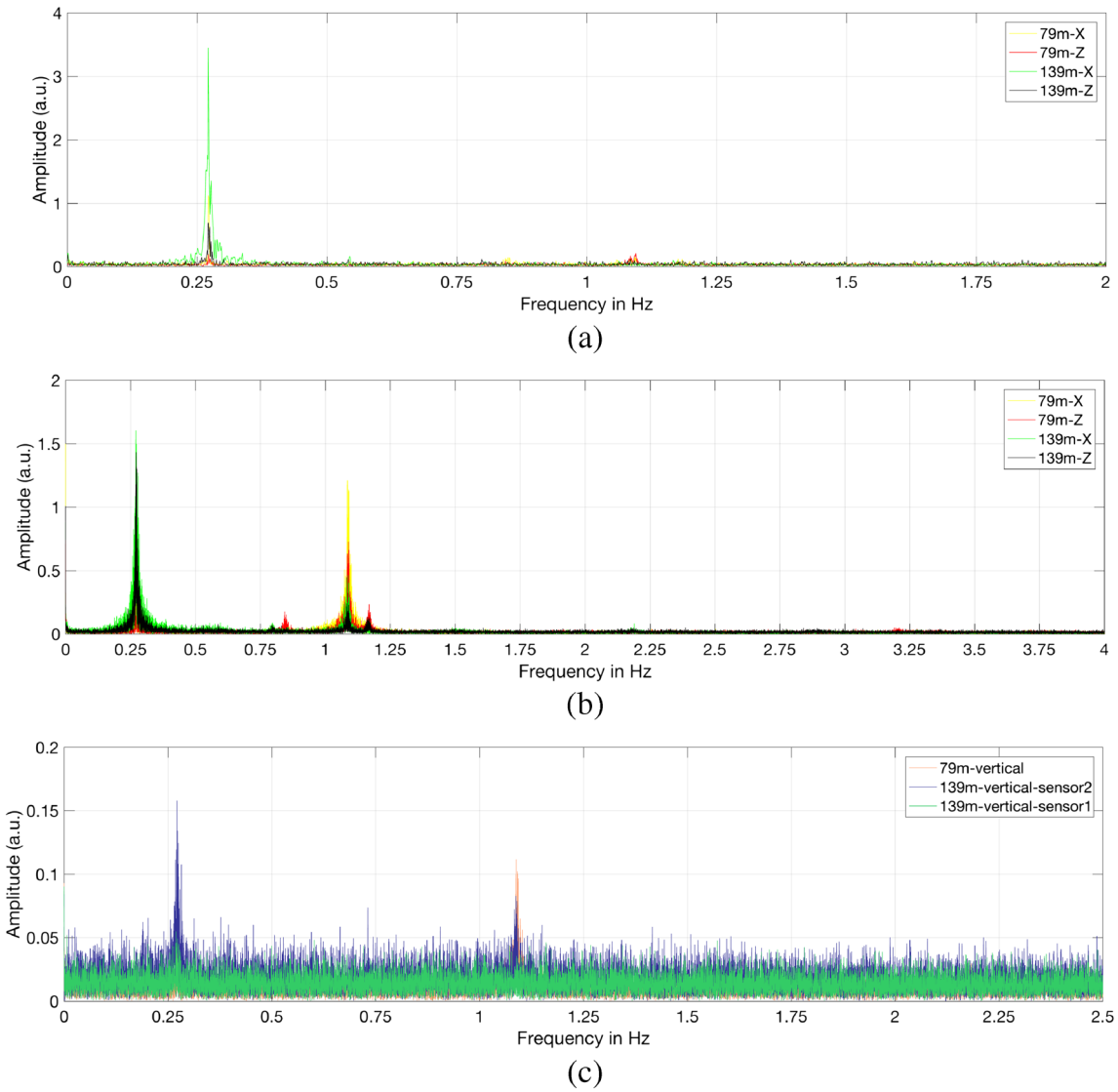

Fig. 9 Frequency spectra derived from measurements of first sensor node generation: **a** frequencies in horizontal directions during first period, **b** frequencies in horizontal directions during second period, and **c** frequencies in vertical direction during second period

3D wireless sensor nodes to the wire-based 1-axis acceleration sensors with higher sampling rate (1 kHz), but lower resolution of 0.1 mg. Frequency spectra were derived both from accelerations values of the wire-based accelerometers (Fig. 10a) and the wireless sensor nodes (Fig. 10c). The displayed load condition was a frequency sweep of the eccentric motor from 1 to 3 Hz and a frequency sweep of the sine wave generator from 4 to 12 Hz with a force of 490 N. These

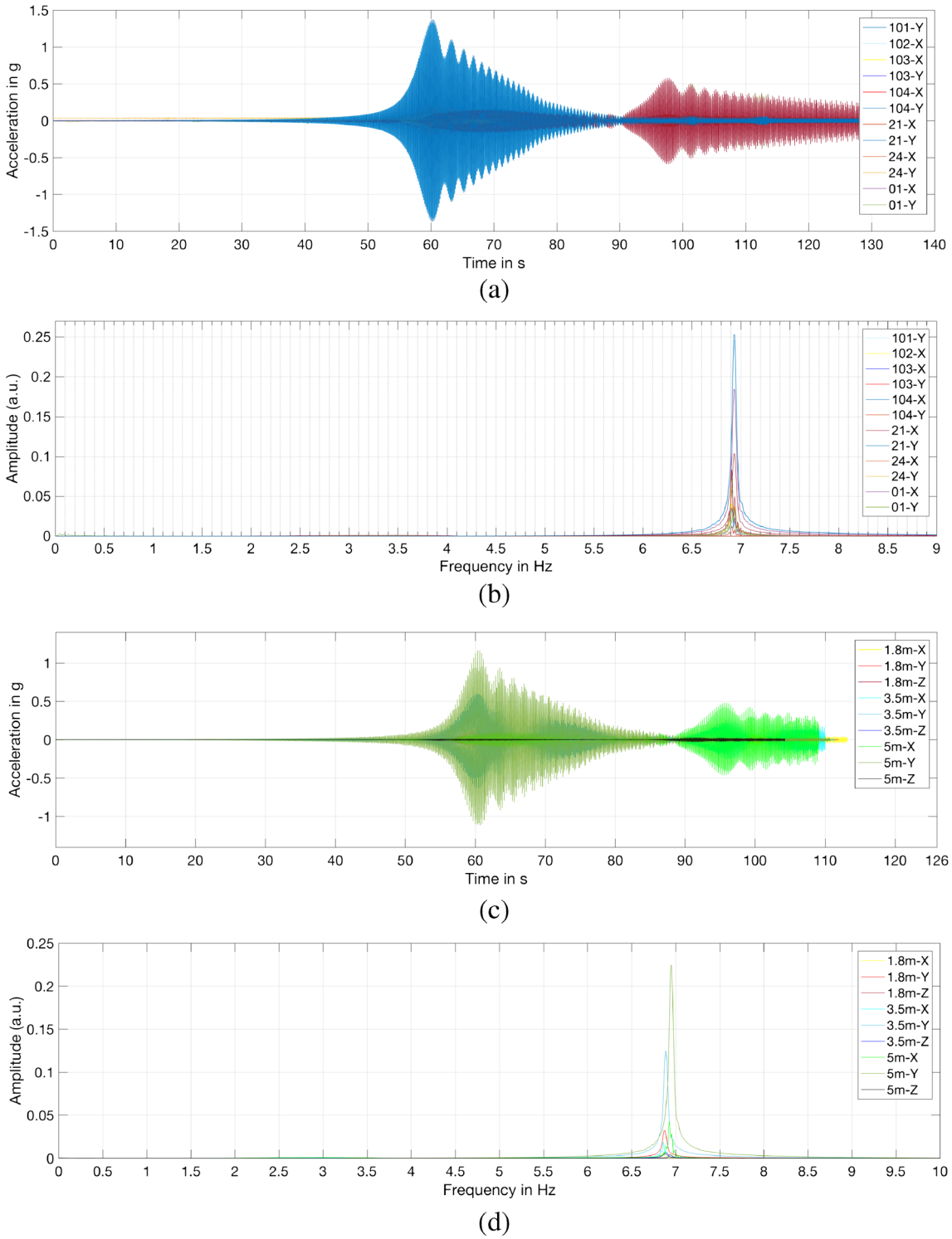

Fig. 10 Acceleration recordings at vibration test system: **a** accelerations measured by wire-based sensors across time, **b** frequency spectra derived from wire-based sensor measurements, **c** accelerations measured by wireless sensor nodes second generation across time, and **d** frequency spectra derived from acceleration measurements by wireless sensor nodes second generation

two sweeps were phase-shifted to each other. As Fig. 10 b and d show, charts of both sensor types indicate a steel tube eigenfrequency of 6.9 Hz.

Results from Measurement Campaign of Wireless Sensor Nodes Second Generation at Wind Turbine

Due to the higher sensitivity of the sensor nodes of the second generation, the wind speed of 5 to 11 m/s and the additional sensor location at the intermediate steel platform, the FFT of the recorded acceleration values generated frequency spectra with several frequency peaks, as shown in Figs. 11 and 12.

The most significant frequency peaks were found at 0.23 Hz, 0.27 Hz, 0.7 Hz, 1.09 H, and 3.3 Hz. For better comparison and analysis of the signals, the frequency spectra were displayed in separate charts according to the axis direction (X, Y, Z). For Fig. 10a, b, and c, the displayed frequency ranges are limited to 0–1.5 Hz.

The rotational frequency of the turbine (0.23 Hz, 1p) and the first bending frequency (0.27 Hz) are most dominant in the spectra from the sensor node on the nacelle platform (Fig. 11a, b, c). The blade passing frequency (3p) of 0.7 Hz shows equivalent amplitudes for the sensor nodes on nacelle platform and intermediate steel platform. The second bending frequency of 1.09 Hz is dominant in the spectra of the sensor nodes at the adapter platform and the intermediate steel platform.

Figure 12a, b, and c show the sections of the frequency spectra from 1.5 to 6 Hz. The frequency peak at 3.3 Hz is interpreted as the third bending frequency, the highest amplitudes of the frequency spectra in horizontal directions are from the sensor node at the intermediate steel platform. At the spectra derived from vertical accelerations, the sensors from all three platforms measure similar amplitudes at 3.3 Hz.

There are indications of eigenfrequencies higher than 3.3 Hz, but they feature either a low signal-to-noise ratio or do not appear in both horizontal dimensions. This will be studied in detail during further measurement campaigns.

Results from Comparison of Wireless Sensor Nodes Second Generation to Installed Wire-Based Sensors at Wind Turbine

As the acceleration signals during measurement campaign on 28 March 2018 from the wireless sensors of second generation and the wire-based sensors were found to be consistent, a consistency of the derived frequency spectra was expected. Figure 13 shows the frequency

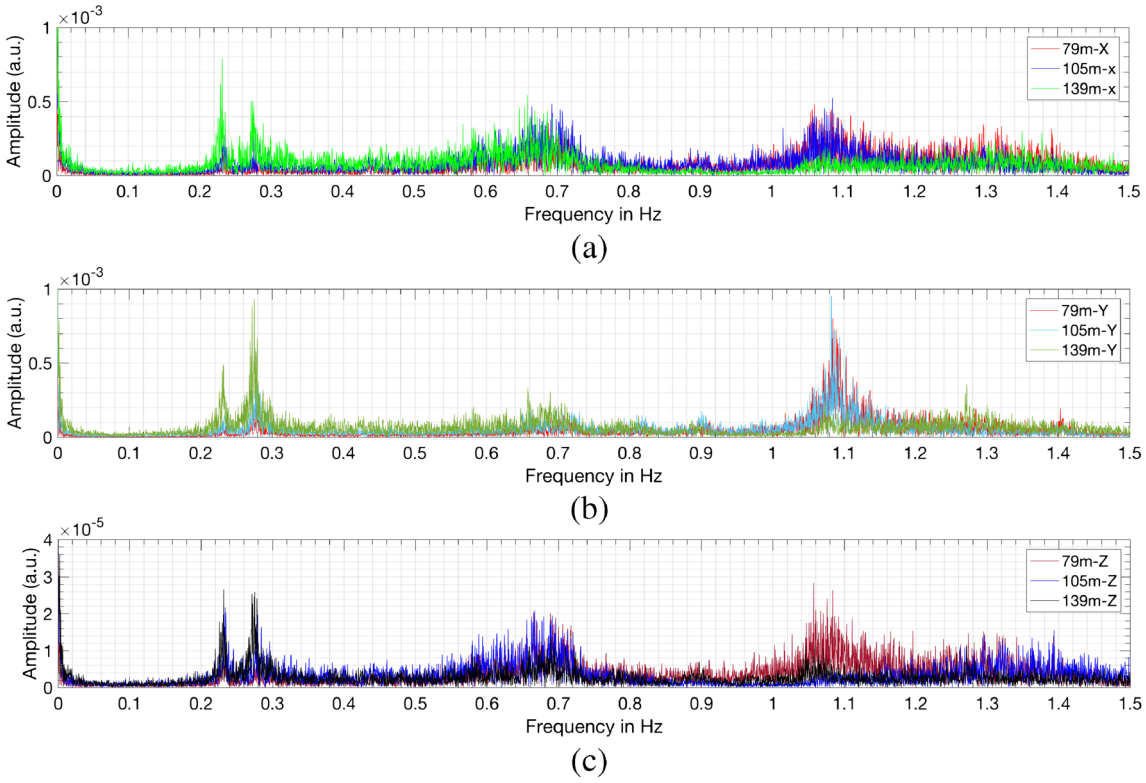

Fig. 11 Frequency spectra derived from first period, limited to frequency range 0–1.5 Hz at three platforms (79 m, 105 m, 139 m): **a** *X*-direction, **b** *Y*-direction, and **c** *Z*-direction

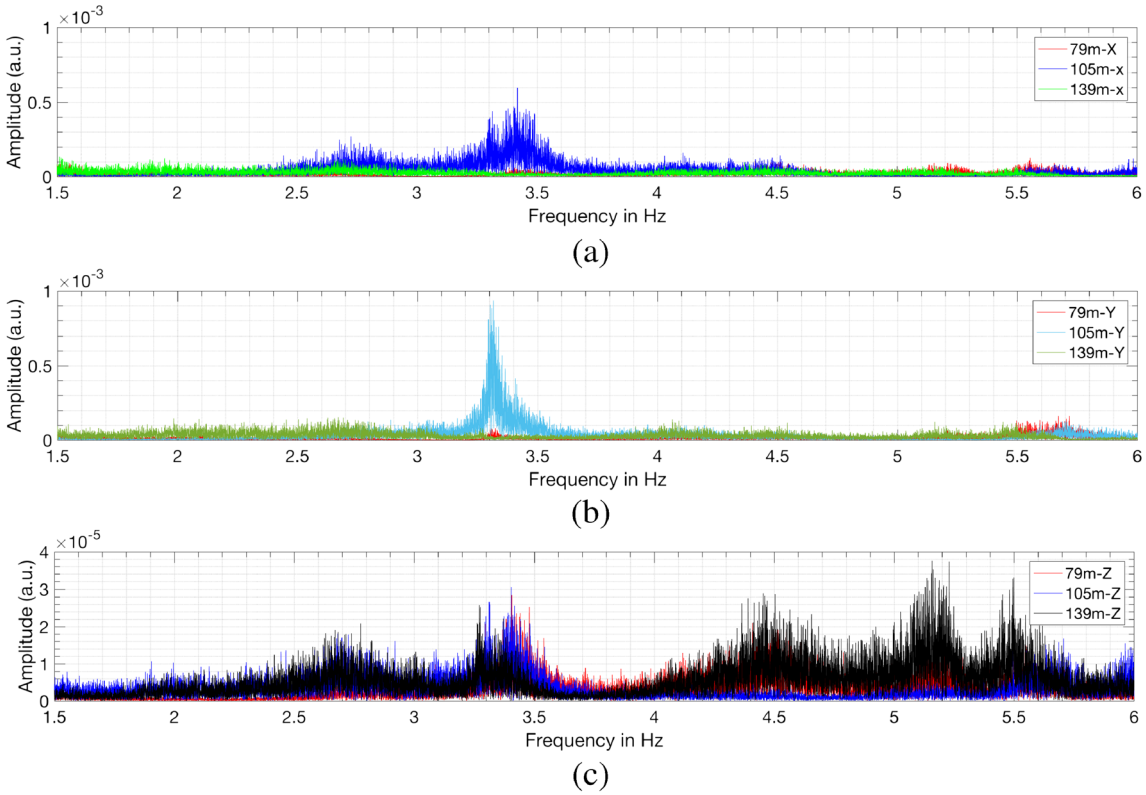

Fig. 12 Frequency spectra derived from first period, limited to range 1.5–6 Hz at three platforms (79 m, 105 m, 139 m): **a** *X*-direction, **b** *Y*-direction, and **c** Z-direction

spectra, derived by FFT from the acceleration signals in horizontal *Y*-direction of one wireless sensor and its wire-based counterpart, both mounted at the adapter platform 79 m above ground. Within the frequency range from 0 to 1.5 Hz (Fig. 13a), both spectra derived from the wireless sensor signals respectively the wire-based sensor signals are very similar. Peaks at the frequencies of 0.27 Hz and 1.09 Hz can be seen, while the amplitude at 1.09 Hz is significantly larger than the one at 0.27 Hz. The impact of the second bending mode on the sensors at the adapter platform is dominant, compared to the impact of the first bending mode. Within the range from

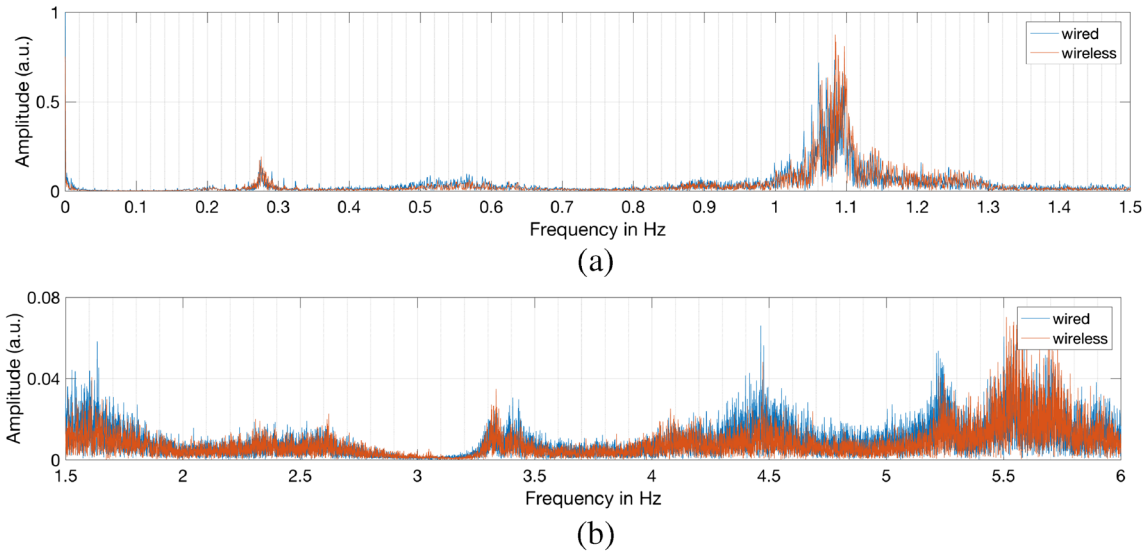

Fig. 13 Frequency spectra derived from wired and wireless sensor measurements on 28 March 2018, *Y*-direction, wind turbine 79-m height, *Y*-direction: **a** limited to range 0–1.5 Hz and **b** limited to range 1.5–6 Hz

1.5 to 6 Hz (Fig. 13b), all peaks are one order of magnitude smaller than the peak of the second bending frequency. Both spectra show peaks at 1.6 Hz, 3.2–3.3 Hz, 4.4 Hz, 5.2 Hz, and 5.6 Hz. There is a discrepancy between the frequency peaks at the expected third bending eigenfrequency. While the spectrum derived from the wireless sensor signals indicates a peak at 3.3 Hz, the spectrum derived from the wire-based sensor signals indicates a peak at 3.4 Hz. In order to exclude a side effect caused by the loss of transmitted data during the first measurement period, the vibration spectra from the wireless sensor nodes for the first measurement period and the second measurement period were compared, as the loss during the second period was only 0.1% of the data. Both spectra show a frequency peak at 3.3 Hz.

Conclusions

Wireless acceleration measurement sensor nodes of two different resolution levels were utilized to monitor the response of a wind turbine tower to wind forces. A data compression algorithm was embedded into the sensor software to support the simultaneous transmission of raw data from several nodes in three dimensions each and to reduce loss of data during transmission. For validation of the recorded acceleration signals, the wirelessly recorded data was compared to acceleration signals recorded by wire-based high-resolution sensors. The following conclusions can be drawn:

1. An acceleration resolution of 1 mg can be insufficient to analyze the behavior of wind turbine towers. At low wind speeds, the acceleration of the tower is within the same order of magnitude as the sensor resolution. Discretization steps can be seen in the recordings and higher vibration frequencies cannot be analyzed with a suitable signal-to-noise ratio.
2. The acceleration resolution of 4 μg is sufficient, even if the system resolution is one order of magnitude higher than the resolution of the sensor chip only. Higher bending frequencies can be analyzed and its amplitude compared to each other. Impacts of vibrational modes depend on the position along the *Z*-axis of the tower. The sensor at the nacelle platform experienced highest impact from the first bending mode while the intermediate steel platform and the adapter platform experienced highest impact from the second bending mode. The amplitude at the frequency of 3.3 Hz is high for the spectrum derived from the sensor signals at the intermediate platform, but low for the spectra derived from sensors at the other two platforms. Even the peak of the rotational frequency at 0.23 Hz (1p) is shown which could not be detected by the wireless sensor of first generation.
3. The comparison of data from the wireless sensors to data from wire-based sensors has proven an equivalence of the monitoring process. Time series of acceleration signals were consistent and derived frequency spectra showed good accordance, both during high acceleration up to 1.5 g at the vibration test station and during low acceleration at the turbine tower.

Based on these findings, wireless acceleration measurement sensors of second hardware generation are considered to be suitable for monitoring of wind turbine towers. Further objectives will be the search for the most suitable algorithm to extract modal parameters and subsequently the integration of such algorithm into the firmware on the sensor chip. By this measure, only the key information will be transmitted to the gateway and battery lifetime can be extended. Higher sampling rates of the wireless sensors beyond 31 Hz can be applied and more than three sensors can be utilized at the same time as the transmission of the key information requires far less bandwidth and the present limit of 320 Hz at the receiving gateway is not a critical limit anymore. Next-generation firmware should operate autonomous and start permanent sampling only if a predetermined acceleration threshold is exceeded. Finally, sophisticated frequency-based data compression techniques and setup of comprehensive wireless sensor network for wind turbine monitoring will be the subject of future work.

Acknowledgments The authors want to thank the German Federal Ministry for Economic Affairs and Energy for funding the project as part of the MISTRALWind project. The authors also want to thank all project partners of the MISTRALWind project, particularly IABG and MAX BÖGL for their support during the measurement campaigns.

Author contributions B. Wondra performed the experiments with the wireless sensors and analyzed the data, S. Malek generated and optimized the software for the wireless sensors and wrote the section 2.2.2 (data compression technique), M. Botz performed the experiments with the wire-based sensors installed at the wind turbine and wrote the corresponding section; M.Botz, S. Glaser and C. Grosse helped in analysis of the recorded and transformed signals, and B. Wondra wrote the manuscript.

Restriction on data availability The acceleration measurement data recorded by the wire-based sensors of IABG at the vibration test station (section "Results from Measurement Campaign of Wireless Sensor Nodes Second Generation at Vibration Test Station" of manuscript) cannot be released without prior consent of IABG. The acceleration measurement data recorded at the studied wind turbine (sections "Comparison to Installed Wire-Based Accelerometers" and "Results from Comparison of Wireless Sensor Nodes Second Generation to Installed Wire-Based Sensors at Wind Turbine" of manuscript) cannot be released without prior consent of MAX BÖGL.

Compliance with ethical standards

Conflicts of interest The authors declare that they have no conflict of interest.

References

1. Global Wind Statistics 2017. Available online: http://gwec.net/wp-content/uploads/vip/GWEC_ PRstats2017_EN-003_FINAL.pdf (accessed on 23 June 2018)
2. Wind in power 2017. Annual combined onshore and offshore wind energy statistics. Wind Europe. Available online: https://windeurope.org/wp-content/uploads/files/about-wind/statistics/WindEurope- Annual-Statistics-2017.pdf (accessed on 23 June 2018)
3. Geiss, C.T.; Kinscherf, S.; Decker, M.; Romahn, S.; Botz, M.; Raith, M.; Wondra, B.; Grosse, C.U.; Osterminski, K.; Emiroglu, A.; Bletzinger, K.-U.; Obradovic, D.; Wever, U. The Mistralwind project—towards a remaining useful lifetime analysis and holistic asset management approach for more sustainability of wind turbine structures. In Proceedings of 11th International Workshop on Structural Health Monitoring (IWSHM), Stanford, CA, USA, September 2017
4. C.T. Loraux, C. Brühwiler, The use of long term monitoring data for the extension of the service duration of existing wind turbine support structures. J. Phys. Conf. Ser. **753**(7) (2016). https://doi.org/10.1088/1742-6596/753/7/072023
5. C.T. Loraux, in *Lausanne*. Long-term monitoring of existing wind turbine towers and fatigue performance of UHPFRC under compressive stresses, PhD thesis, EPFL (February 2018)
6. N. Noppe, W. Weijtjens, C. Devriendt, Modeling of quasi-static thrust load of wind turbines based on 1 s SCADA data. Wind Energy Science (WES) **3**(1), 139–147 (2018). https://doi.org/10.5194/wes-3-139-2018
7. K. Smarsly, D. Hartmann, K.H. Law, An integrated monitoring system for life-cycle management of wind turbines. Smart. Struct. Syst. **12**(2), 209–233 (2013). https://doi.org/10.12989/sss.2013.12.2.209
8. W. Weijtjens, T. Verbelen, G. De Sitter, C. Devriendt, Foundation structural health monitoring of an offshore wind turbine—a full-scale case study. Struct. Hlth. Monit. **15**(4), 389–402 (2016). https://doi.org/10.1177/1475921715586624
9. R.A. Swartz, J.P. Lynch, S. Zerbst, B. Sweetman, R. Rolfes, Structural monitoring of wind turbines using wireless sensor networks. Smart. Struct. Syst. **6**(3), 183–196 (2010). https://doi.org/10.12989/sss.2010.6.3.183
10. L. Zhu, Y. Fu, R. Chow, B.F. Spencer, J.W. Park, K. Mechitov, Development of a high-sensitivity wireless accelerometer for structural health monitoring. Sensors **18**(1), 262 (2018). https://doi.org/10.3390/s18010262
11. Giurgiutiu, V. Structural health monitoring (SHM) of aerospace composites. In Polymer Composites in the Aerospace Industry; Irving P., Soutis, C.; Woodhead Pub.: Cambridge, UK, 2014; 449–507, ISBN 978-0-85709-523-7
12. A.K. Pandey, M. Biswas, M.M. Samman, Damage detection from changes in curvature mode shapes. J. Sound Vib. **145**(2), 321–332 (1991). https://doi.org/10.1016/0022-460X(91)90595-B
13. El-Kafafy, M.; Colanero, L.; Gioia, N.; Devriendt, C.; Guillaume, P.; Helsen, J. Modal parameters estimation of an offshore wind turbine using measured acceleration signals from the drive train. In Structural Health Monitoring & Damage Detection; Niezrecki, C.; Springer International Publishing, Cham, Switzerland, 2017, Volume 7, 41–48, ISBN 978–3–319-54109-9
14. D. Duckwitz, M. Shan, in *Proceedings of the Special Topic Conference: The Art of Making Torque from Wind, Oldenburg*. A survey on control concepts for the reduction of tower loads (conference poster) (October, Germany), p. 2012
15. Kim, S.; Pakzad, S.; Culler, D.; Demmel, J.; Fenves, G.; Glaser, S.; Turon, M. Health monitoring of civil infrastructures using wireless sensor networks. In Proceedings of the 6th International Conference on Information Processing in Sensor Networks, Cambridge, MA, USA, 254–263 April 2007
16. ADXL362 Data Sheet Rev. E. Analog Devices Inc., (2016). Available online: http://www.analog.com/en/ products/sensors-mems/accelerometers/adxl362.html (accessed on 23 June 2018)
17. ADXL354/ADXL355 Data Sheet Rev. A. Analog Devices Inc., (2018). Available online: http:// www.analog.com/en/products/sensors-mems/accelerometers/adxl355.html (accessed on 23 June 2018)
18. Pelkonen, T.; Franklin, S.; Teller, J.; Cavallaro, P.; Huang, Q.; Meza, J., Veeraraghavan, K. Gorilla: a fast, scalable, in-memory time series database. In Proceedings of the 41st International Conference on Very Large Data Bases, Kohala Coast, Hawaii, USA, 1816–1827 August 2015
19. Botz, M.; Oberlaender, S.; Raith, M.; Grosse, C. U. Monitoring of wind turbine structures with concrete-steel hybrid-tower design. In Proceedings of the 8th European Workshop on Structural Health Monitoring (EWSHM), Bilbao, Spain, 2301–2311 July 2016
20. Botz, M.; Raith, M.; Emiroglu, A.; Grosse, C.U. Monitoring of wind turbine structures using stationary sensors and short-term optical techniques. In Proceedings of the 11th International Workshop on Structural Health Monitoring (IWSHM), Stanford, CA, USA, 2519–2521 September 2017
21. Botz, M.: Zhang, Y.; Raith, M.; Pinkert, K. Operational modal analysis of a wind turbine during installation of rotor and generator. In Proceedings of the 7th International Operational Modal Analysis Conference (IOMAC), Ingolstadt, Germany, 224–227 May 2017